Journal of Controlled Release 365 (2024) 688–702

Contents lists available at ScienceDirect

Journal of Controlled Release

journal homepage: www.elsevier.com/locate/jconrel

# pH-dependent pressure-sensitive colonic capsules for the delivery of aqueous bacterial suspensions

Fatma Abdi [a], Marina Green Buzhor [a], Nadia Zellweger [a], Zhi-Luo [b], Jean-Christophe Leroux [a,*]

[a] Institute of Pharmaceutical Sciences, Department of Chemistry and Applied Biosciences, ETH Zürich, 8093 Zürich, Switzerland
[b] Department of Biomedical Engineering, Southern University of Science and Technology, 518055 Shenzhen, Guangdong, China

ARTICLE INFO

*Keywords:*
Microbiome
Pressure capsules
Aqueous suspensions
Colonic delivery
Live bacteria

ABSTRACT

Microbiome-based therapies hold great promise for treating various diseases, but the efficient delivery of live bacteria to the colon remains a challenge. Furthermore, current oral formulations, such as lyophilized bacterial capsules or tablets, are produced using processes that can decrease bacterial viability. Consequently, high dosages are required to achieve efficacy. Herein, we report the design of pressure-sensitive colonic capsules for the encapsulation and delivery of aqueous suspensions of live bacteria. The capsules consisted of 2 functional thin-films (hydrophobic and enteric) of ethyl cellulose and Eudragit S100 dip-coated onto hydroxypropyl methylcellulose molds. The capsules could be loaded with aqueous media and provide protection against acidic fluids and, to some extent, oxygen diffusion, suggesting their potential suitability for delivering anaerobic bacterial strains. Disintegration and mechanical studies indicated that the capsules could withstand transit through the stomach and upper/proximal small intestinal segments and rupture in the ileum/colon. *In vitro* studies showed that bacterial cells (anaerobic and aerobic commensals) remained highly viable (74–98%) after encapsulation and exposure to the simulated GI tract conditions. *In vivo* studies with a beagle dog model revealed that 67% of the capsules opened after 3.5 h, indicating content release in the distal gastrointestinal tract. These data demonstrate that live aqueous bacterial suspensions comprised of both aerobic and anaerobic commensals can be encapsulated and in the future might be efficiently delivered to the distal gastrointestinal tract, suggesting the practical applications of these capsules in microbiome-based therapies.

## 1. Introduction

Microbiomics is gaining attention due to new insights into the relationship between microbiota and homeostasis. [1] Human microbiota modulate many important functions and biological pathways ranging from the immune system to metabolism. [2,3] For example, it has been observed that patients who received an antibiotic treatment alone responded less effectively to immunotherapy than groups that received a fecal microbiota transplant (FMT) post antibiotic treatment. [4] Indeed, the presence of defined bacterial taxa, which secrete certain metabolites, improved the therapeutic response. FMT has also shown efficacy in combating recurrent *Clostridium difficile* infections, resulting in the recent approval of the first FMT therapy (REBYOTA©). [5] However, FMT is mainly achieved through single/multiple treatments of small intestinal infusion *via* a nasoduodenal tube, colonoscopy, or a colonic retention enema, which are usually uncomfortable for patients and necessitate the intervention of a clinician. [6,7] In this respect, more conventional dosage forms, such as tablets and capsules, are preferred for administering bacterial cultures.

Although capsules and tablets offer numerous benefits for biologics delivery, encapsulating and delivering biologics through these forms presents several challenges that must be overcome. First, certain steps involved in the production of these formulations (*e.g.*, freeze-drying, compaction, and processing) can significantly reduce bacterial survival. [8–12] For instance, the pressure exerted during tableting can reduce viability by 80%, leading to the administration of high doses to compensate for bacterial loss. [13] Second, many physiological barriers must be overcome for the bacteria to reach the ileum or colon, where the intestinal microbiome resides, in a viable state. Indeed, the harsh environment of the gastrointestinal (GI) tract, such as the acidity of the stomach as well as the presence of digestive enzymes (*e.g.*, pepsin, pancreatin) and bile acids in the small intestine, makes the oral delivery of living organisms challenging. [14–17] In addition, many beneficial bacterial strains are strictly anaerobic, requiring protection from

* Corresponding author.
*E-mail address:* jleroux@ethz.ch (J.-C. Leroux).

https://doi.org/10.1016/j.jconrel.2023.11.048
Received 14 June 2023; Received in revised form 21 November 2023; Accepted 24 November 2023
Available online 7 December 2023

environmental oxygen. [18] Despite the difficulty of these challenges, some of them can be partially overcome through the use of enteric formulations (which afford protection from gastric fluids) or bacterial spores (*e.g.*, SER-109 for treating *C. difficile* infection). [19–22] However, to increase bacterial resistance, sporulation is not always possible, and often large doses of microorganisms need to be administered to compensate for viability loss. [23] One possible approach for reducing dosage is to omit the drying step and deliver live bacteria as encapsulated aqueous suspensions. While the administration of FMT with capsules has been reported, the formulation was not specifically designed for aqueous suspensions and had to be quickly frozen to prevent leakage. [24]

Since most oral formulations are in some respects sensitive to water, delivering aqueous media is somewhat challenging but might be achieved through the use of pressure-controlled delivery capsules (PCDCs), which break when exposed to the increase in internal pressure in the colon during stool formation. [25] PCDCs are generally composed of ethyl cellulose (EC) and optional enteric polymers and have been tested with various drugs (*e.g.*, 5-aminosalicylic acid, tegafur, carbamazepine) dispersed in suppository bases or solvents (*e.g.*, low-molecular-weight poly(ethylene glycol)). [26–28] Moreover, PCDCs have also been used to deliver an aqueous solution of glycyrrhizin disodium salt to the colon in a beagle dog model. [29] While the manufacturing process allowed for the preparation of individual capsules, it was quite complex. Gelatin capsules' parts were sealed with EC, holes were added on the top and bottom of the glued parts and used to introduce a solution of EC dissolved in organic solvents and evaporated under rotation for 10 h at 40 °C. After evaporation, the solution of glycyrrhizin was added and the holes consequently sealed. [28] For this reason, alternative production methods, such as dip-coating, were explored in subsequent studies. However, sealing the capsules led in some cases, *in vivo,* to non-disintegration of the dosages retrieved intact in the feces or premature pinhole formation leading to the appearance of fluorescein in the serum prior to colonic arrival. [30]

Inspired by PCDCs, we report a pressure-sensitive colonic capsule for the oral administration of unprocessed aqueous bacterial suspensions (Fig. 1). The capsule, prepared with the dip-coating method and locked *via* a coni-snap mechanism, is composed of an inner pressure-sensitive thin hydrophobic polymeric membrane, which allows the encapsulation of aqueous media. To avoid premature shell rupture prior to reaching the distal GI tract and protect the live biologics from the acidic gastric environment and duodenal/jejunal fluids (which contain digestive enzymes and bile acids), the capsules are mechanically reinforced by an enteric coating that dissolves at pH values above 7 (Fig. 1).

Upon reaching the ileum/colon, the loss of the enteric coating would lead to a loss of mechanical strength favorizing the mechanical rupture of the thin hydrophobic coating and the release of the capsule content.

## 2. Materials and methods

### 2.1. Materials

Ethyl cellulose (EC) (300 cps with a 48% ethoxy substitution), sodium chloride (NaCl), indigo carmine, sodium thiosulfate ($Na_2S_2O_3$), Evans blue, potassium phosphate monobasic ($KH_2PO_4$), sodium hydroxide (NaOH) and bile acids (sodium cholate and sodium deoxycholate) were purchased from Sigma–Aldrich. Ethyl acetate, ethanol and isopropyl alcohol (IPA) were obtained from Acros Organics. Butyl benzoate was purchased from Fluka. Eudragit S100 was obtained from Evonik. Lecithin (from soybean, 90 wt%) was obtained from PanReac Appli Chem. Hydrochloric acid (HCl) was provided by VWR Chemicals. HPMC commercial capsules (size 0) were purchased from Interdelta Switzerland. The Sylgrad™ 184 Silicone Elastomer kit (containing elastomer base and curing agent) was purchased from DOW Europe. Barium sulfate ($BaSO_4$) suspension (Micropaque) was purchased from Guerbet Pharmaceuticals. Carbon steel blades were purchased from Swann-Morton. A sealable cell (117.104-QS), quartz glass (Suprasil, 10 mm Light PathAll) and silicone rubber (septa) were obtained from Altmann Analytik GmbH & Co. KG. LIVE/DEAD™ BacLight™ Bacterial Viability Kit, for microscopy & quantitative assays was purchased from Sigma–Aldrich. Brain heart infusion (BHI) as well as Man–Rogosa–-Sharpe (MRS) powder were obtained from Millipore. Symprove™ bacterial suspension containing four bacterial strains: *Lactobacillus acidophilus* NCIMB 30175, *Lactobacillus plantarum* NCIMB 30173, *Lactobacillus rhamnosus* NCIMB 30174 and *Enterococcus faecium* NCIMB 30176 was ordered directly from the manufacturer (Symprove Ltd., London, England). *Bacteroides thetaiotaomicron* was obtained from Prof. Slack lab. Hemin and cysteine were obtained from Sigma-Aldrich. Stainless-steel metallic pins for coating were custom designed by the ETH physics workshop (Fig. S3 and Table S3). Chemicals were used as received.

### 2.2. Coating and preparation of the composite capsules

Composite capsules were made of a hydrophobic coating (HC-1 and HC-2) and an enteric coating (EnC-1 and EnC-2). Composite capsules, denoted as HC-1 EnC-1 and HC-2 EnC-2 capsules, were created. Briefly, EC (400 or 600 mg) were dissolved in 10 mL of ethyl acetate overnight

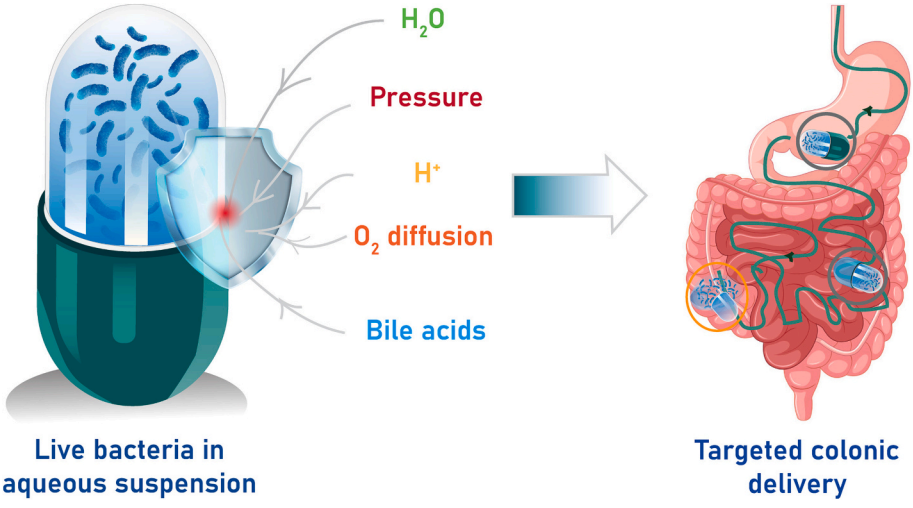


**Fig. 1.** Schematic illustration of the pressure-sensitive capsule containing an aqueous suspension of live bacteria. The capsule protects the bacteria during GI transit and releases its contents through pressure-induced rupture upon reaching the ileum/colon.

under vigorous stirring (1500 rpm) to obtain viscous solutions with 4.5 or 6.6 wt% EC. One layer of 6.6% or 2 layers of 4.5 wt% EC constituted the hydrophobic coating of HC-1 EnC-1 and HC-2 EnC-2, respectively. For the coating step, 3 mL of each solution were transferred into a 4-mL glass flask. Commercially available size 0 HPMC capsules were separated into caps and bodies and then dip-coated either in 4.5 or 6.6 wt% EC solution to obtain the first layer. Coated capsule parts were placed on the designed stainless-steel metallic pins and left to dry at room temperature (RT) for 1 h. Then, the second layer of EC 4.5 wt% was deposited and left to dry for another 30 min at RT. The metallic pins were then transferred to an incubator (37% relative humidity, 27 °C) for further overnight drying. Enteric coatings 1 (EnC-1) and 2 (EnC-2) were prepared as follows: 1 g of Eudragit S100 was vortexed with 0.3 mL or 3 mL of butyl benzoate in a 20-mL glass vial, respectively. Then, the mixture was dissolved overnight in 10 mL (isopropyl alcohol: ethanol) (1:1 v/v). Two layers of EnC-1 or EnC-2 were deposited on either HC-1 or HC-2, respectively, following the same procedure as previously described. The drying procedure was also the same. The final products, HC-1 EnC-1 and HC-2 EnC-2, were stored in an incubator (37% relative humidity, 27 °C) until further use. Body and cap parts were joined and locked like conventional capsules.

### 2.3. Scanning electron microscopy (SEM) and thickness determination

SEM images of HC-1, HC-2, HC-1 EnC-1 and HC-2 EnC-2 capsules were obtained. Due to the hollowness and thinness of the coatings, the capsules were filled with polydimethylsiloxane to facilitate cutting and preserving the structure. To this end, the Sylgrad 184 Silicone elastomer kit was used. Briefly, 10 g of silicon elastomer base and 1 g of its curing agent were mechanically mixed in a 20 mL glass vial with a spatula until the viscosity decreased. Six hundred μL of this mixture were poured into the capsule, which were fully locked and placed vertically into a vacuum chamber. Vacuum (down to $10^{4}$ Pa) was applied 3 times to remove internal air bubbles. Thereafter, the capsules were cured at 80 °C overnight. A carbon steel blade was used to obtain cross sections for SEM imaging. The sample morphology and thickness of the coatings were characterized with a field emission scanning electron microscope (JSM 7100F, JEOL Ltd.) in secondary and backscattered electron modes. The samples were mounted on metallic stubs using conductive carbon cement (Leit-C, Plano GmbH, Wetzlar). The samples were coated with 5 nm carbon using a carbon coater (CCU-010, Safematic GmbH, Zizers). Cross-section images of the coatings were obtained at an acceleration voltage of 3.0 kV and a 15.00 mm working distance. Capsules were analyzed, images were taken, and the thickness of each coating layer was determined using ImageJ.

### 2.4. Contact angle determination

HC-1, HC-2, EnC-1 and EnC-2 capsules were used for these experiments. Freshly prepared capsules were cut diametrically with a scalpel and opened to form a long rectangular layer. This layer was fixed on a 2-faced tape and glued on the platform of the contact angle goniometer (DSA100, Krüss Scientific) equipped with Image Analysis Software (IAS) (DSA4, Krüss Scientific). The IAS used a digital video camera to scan an image of the drop and automatically calculated both the left and right contact angles and drop dimension parameters from the digitalized image. Static contact angles were recorded on the coated side of the capsule, and water was used as a liquid. A volume of 6–7 μL was used to determine the contact angle.

### 2.5. Raman spectroscopy

Raman spectra of the initial materials (EC, HPMC and Eudragit S100) were acquired using a confocal Raman spectrometer (Horriba LabRAM HR Evolution UV-VIS-NIR). A few milligrams of Eudragit S100, HPMC or EC were placed on a glass slide, and a 297-mW 785-nm diode laser excitation source was used to excite the sample through a 50× objective. The recorded spectral range was 150–3250 $cm^{-1}$ using a 300 g/mm grating at 600 nm, while the total data acquisition time was 30 s per spectra. Capsule samples were prepared as described for SEM imaging. Parameters to map the capsule samples were kept the same as those for the polymeric materials; however, a 10× objective was used, and the recorded spectral range was 200–2000 $cm^{-1}$. A 2D scan was performed with a 10-μm step in the y direction (starting from the surface and moving vertically toward the center). While the y position was fixed, 3 spectra in the x direction were obtained by scanning with a 5-μm step (horizontally), and their average was compiled. The average spectra per y position were normalized, and their baseline was adjusted. Then, the signals at 244, 289 and 1719 $cm^{-1}$ representing EC, HPMC and Eudragit S100, respectively, per y position were collected and normalized again using Origin (Origin version 2021).

### 2.6. Proton diffusion determination

HC-1, HC-2, HC-1 EnC-1 and HC-2 EnC-2 capsules were used for these experiments. A glass bath container was filled with simulated gastric fluid (SGF) and heated to 37 °C under magnetic stirring (100 rpm). SGF was prepared accordingly: 4 g of NaCl were dissolved in 2 L of Milli-Q water, and the pH was adjusted with HCl (12 M) to obtain a pH of 1.2. A 3D-printed holder with 9 holes corresponding to the diameters of the capsules was created, and a temperature probe was fixed on it (Fig. S4). Then, 3 capsules per group were inserted into the holder and filled with 600 μL of deionized water (DW). The platform was suspended on SGF (3/4 of capsule height was immersed). The capsule inner pH was determined with a microelectrode (pH electrode InLab Micro, Mettler Toledo) over a 4-h period, and measurements were taken every 15 min. Nine capsules per group were analyzed. All proton diffusion data reported in the Supplementary Results were obtained in an identical fashion.

### 2.7. Oxygen diffusion determination

Indigo carmine was used to monitor the oxygen content inside the capsules. Briefly, 25 mg of indigo carmine were dissolved in 100 mL of DW, which was further diluted (1:1 (v/v)). Then, 6.8 mL of this solution were added to 6 mL of DW in a 20-mL glass vial closed with a septum. The solution was degassed under argon (Ar) for 30 min to remove the oxygen. Sodium thiosulfate $Na_2S_2O_3$ (2.25 g/L, 250 μL) were added to the probe solution under Ar, resulting in the working solution, which turned from blue to colorless/yellowish instantaneously.

Calibration Curve. A quartz cuvette was prepared by closing it with a silicon septum and then flushing it with Ar gas. Next, 550 μL of the working solution were added to the cuvette in an Ar environment. To create a blank, 170 μL of degassed DW were added to the cuvette. The cuvette was then manually agitated for 1 min to ensure thorough mixing. Absorbance spectra were recorded between 420 and 800 nm. These steps were repeated for each calibrator by introducing varying volumes of atmospheric air (ranging from 0.1 mL to 1 mL) into the cuvette using a syringe before shaking the cuvette.

Capsule Oxygen Content. Capsules were filled with Ar-degassed DW and locked. The capsules were then kept under ambient conditions for different time intervals (0, 2, 6, 8, or 24 h). To measure the amount of dissolved oxygen inside the capsules, the capsules were placed in Eppendorf tubes, and 170 μL of Ar-degassed water were placed on top of the capsule. The Eppendorf tubes were then closed under Ar flow, and the capsules were broken by centrifugation (18,000 *xg*, 21 °C, 20 min). The solid parts of the capsules were removed under Ar, and the remaining solution was centrifuged under the same conditions for 10 min. The oxygen concentration in the solution was measured using the previously described method, except that 170 μL of the capsule content were pipetted under Ar atmosphere.

Oxygen content after SGF exposure for 2 h was determined as

previously stated, however capsules (3 per type) were incubated for 2 h in 10 mL SGF at 37 °C and 210 rpm prior to measurement.

### 2.8. Surface dissolution imaging

SGF pH 1.2 was prepared according to the United States Pharmacopeia (USP). Simulated intestinal fluid (SIF) (pH 7.3) was prepared accordingly: Briefly, 13.6 g of potassium phosphate monobasic ($KH_2PO_4$) and 2 g of NaOH were added to 2 L of ultrapure water and stirred until complete dissolution. Capsules were prepared as stated previously. Fig. 6a describes the setup and capsule placement in the whole dosage cell, the direction of circulation of the fluid and the measurement zone. First, glass beads were introduced inside the dosage cell (to reduce turbulence), and the latter was connected to the fluid lines. A washing step was performed automatically with DW prior to measurements. Then, background imaging as well as light emitting diodes calibration was performed with SGF or SIF. When the whole cell was ready, the capsule was filled with 600 μL of DW and fully locked. The sample was then loaded inside the cell using a metallic wire. Capsules were subjected to either SGF or SIF for 2 and 6 h, respectively. The release of butyl benzoate was recorded at 255 nm, and the capsule physical state was imaged at 520 nm. The flow rate and temperature in all steps were set to 15 mL/min and 37 °C, respectively. A closed loop (200 mL) was used during the experiments where the same fluid was introduced over time. Videos of the dissolution experiments were taken for each capsule type.

### 2.9. Disintegration test coupled with mechanical compression

SGF pH 1.2 and SIF pH 7.3 were prepared as described above. SIF pH

a


b

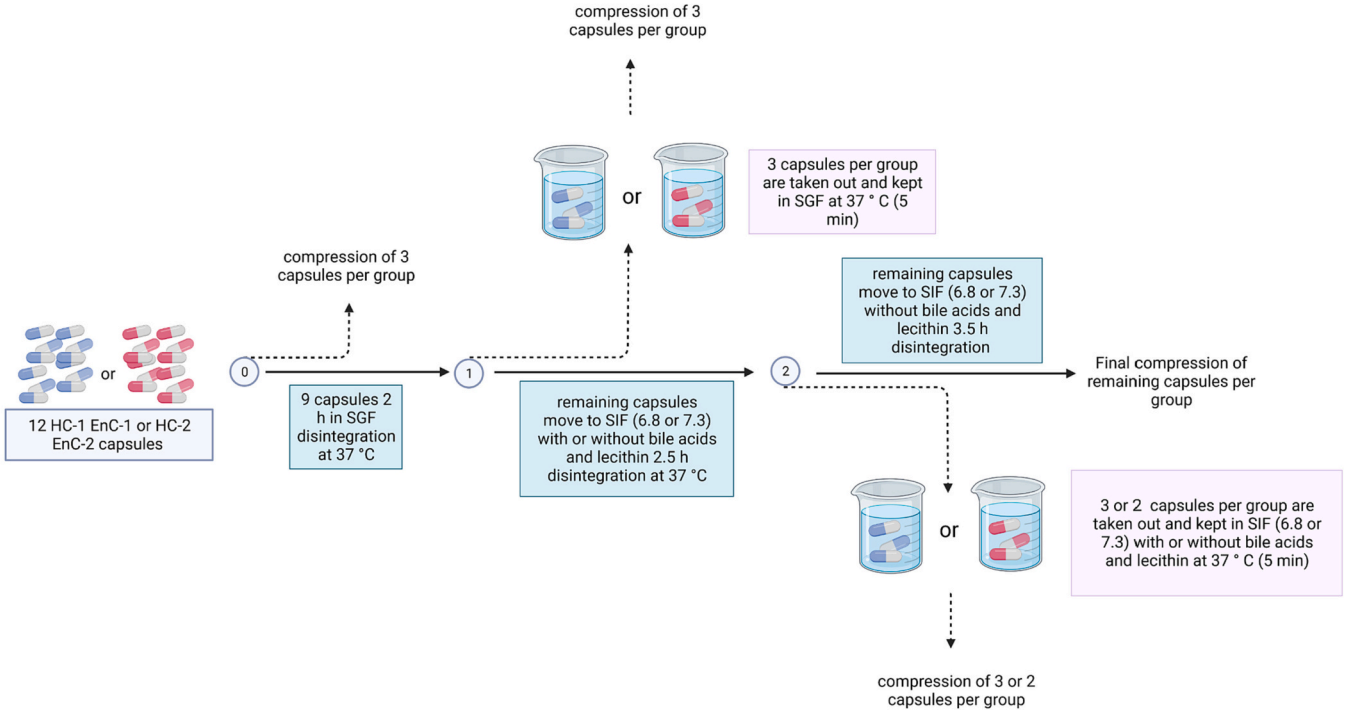


**Fig. 2.** Compression direction during compression test (a) experimental procedure of the disintegration of capsules coupled with compression tests, number of capsules per step and conditions (b). Fig. 2b was created with BioRender.

6.8 was prepared according to the United States Pharmacopeia (USP). Briefly, 13.6 g of potassium phosphate monobasic ($KH_2PO_4$) and 1.8 g of NaOH were added to 2 L of Milli-Q water and stirred until complete dissolution. For some experiments, SIF was supplemented with bile acids (sodium cholate and sodium deoxycholate) (5 mM) and lecithin (0.2 mM). Upon the addition of bile acids and lecithin, the buffers were stirred vigorously (1500 rpm) until complete dissolution and were used fresh. This supplemented SIF appears with a (+) sign.

All disintegration tests (Model E, Erweka) were performed at 37 °C and a movement of 50 cycles/min. Compression tests were performed using an AGS-X (Shimadzu) universal testing machine with a 100-N capacity load cell. All compression test speeds were set as 1, 0.20, and 10 mm/s for the pre, test- and post-tests, respectively. The applied force as a function of distance was collected. To start the recording of the curve, the trigger force was set to 0.049 N to consider minimal forces that might deform soft surfaces such as hydrated capsules. The compression direction was applied as shown in Fig. 2a.

Disintegration tests coupled with mechanical compression as well as the experimental conditions are described in Fig. 2b and Fig. 7. Briefly, 12 capsules per group (HC-1 EnC-1 or HC-2 EnC-2) per experiment were filled with 600 μL of an Evans blue solution (0.05 g/L). Three capsules were immediately compressed, and the remaining 9 capsules were transferred to the disintegration apparatus containing SGF for 2 h at 37 °C. At the end of the disintegration test, to prevent capsule drying, 3 capsules were removed and transferred to a beaker containing SGF (37 °C) for 5 min and then withdrawn from the fluid and compressed. The remaining 6 capsules (if none opened) were then exposed to SIF (pH 6.8 or 7.3) with or without bile acids and lecithin for 2.5 h (37 °C). At the end of this step, 3 capsules (or 2 if some opened) were removed and transferred to a beaker containing SIF (pH 6.8 or 7.3) (37 °C) for 5 min with or without bile acids and lecithin, quickly withdrawn from the fluid and compressed. The remaining capsules were exposed to SIF (pH 6.8 or 7.3) for 3.5 h without bile acids and lecithin, followed by a final compression test. These durations were chosen based on the length of each segment of the human GI tract. [31].

The pressure-at-break ($P_b$) was calculated with Eq. 1:

$$P_b = \frac{F_{at\ break}}{S_{capsule}} \quad (1)$$

Where $F_{at\ break}$ is the maximum force sustained by the capsule before breakage or burst (value where the force curve reaches its maximum before declining (sign of loss of internal pressure)). $S_{capsule}$ is the ideal surface of contact of the compression motif with the capsule, which is $1.6 \times 10^{-4}$ $m^2$.

### 2.10. Bacterial culture and viability assessment

Saline (0.85% NaCl) was prepared by dissolving 8.5 g NaCl in 1 L of Milli-Q-water. IPA (70%) was prepared by adding 700 mL of IPA to 300 mL of Milli-Q water to obtain 1 L. All simulated gastrointestinal fluids as well as saline were filtered through Vacuum Filtration "rapid"-Filtermax.

Bacterial culture. Fifteen mL of MRS were inoculated with a commercially available bacterial aqueous suspension (*i.e.* Symprove™) containing 4 bacterial strains, namely *Lactobacillus rhamnosus*, *Lactobacillus acidophilus, Lactobacillus plantarum* and *Enterococcus faecium*, and incubated at 37 °C, 210 rpm overnight and a cryostock was created. From this cryostock, these 4 bacterial strains were cultured in 15 mL MRS medium overnight while shaking at 210 rpm at 37 °C. From a cryostock, *Bacteroides thetaiotaomicron* was inoculated under an anaerobic tent in 10 mL of BHI medium supplemented with cysteine (1 g/L) and hemin (250 μg/mL). The bacteria were grown in Hungate tubes overnight at 37 °C at 210 rpm.

Viability assessment with flow cytometry. The overnight cultures were centrifuged for 10 min at 4000 *xg* and the supernatant removed. The cultures were washed by resuspending in 10 mL saline, centrifuging at 4000 *x g* and removing their supernatant. The bacterial cultures were finally resuspended in 10 mL saline and their optical density at 600 nm ($OD_{600}$) measured. For the live, dead, SGF and SIF 6.8 (+) controls, 1 mL of this saturated live culture was suspended in 10 mL of saline or 70% IPA or SGF (pH 1.2, 3 and 5) or SIF 6.8 (+) for 1, 1, 2 and 2.5 h, respectively and shaken at 210 rpm at 37 °C. Post exposure to these conditions, these samples were centrifuged for 10 min at 4000 *xg*, the supernatant discarded and the pellet washed as previously mentioned and resuspended in saline to obtain an $OD_{600} \approx 0.07$ for flow cytometry. Three samples per condition were recorded.

For the encapsulation, 550 μL of the saturated live culture were loaded in the capsules (3 capsules per type) and the latter subsequently subjected to the different simulated GI tract conditions (SGF 1.2 for 2 h and SIF 6.8 (+) for 2.5 h). The capsules content was removed using a syringe, and 100 μL were diluted in 900 μL of saline adjusting the $OD_{600}$ to 0.07. For flow cytometry staining, 1 mL of each sample (with an $OD_{600} \approx 0.07$) was stained with 1 mL of staining solution. The staining solution was prepared from the dead/live bacterial kit where 9 μL of Green Fluorescent Nucleic Acid Stain SYTO9 (3.34 mM) were mixed with 9 μL propidium iodide (20 mM) and 16.5 μL of this mixture was added to 11 mL of sterile water. The flow cytometry density plots were recorded 15 min post staining.

### 2.11. In vivo protocol

This protocol was ethically approved by Shenzhen Advanced Medical Services Co., Ltd and the institutional animal care and use committee (IACUC) under the number AASC211214D. A male Beagle dog, aged 1 year and 1 month, weighing 10 kg, was kept in a fasted state (with free access to water) for at least 12 h before the experiment. Thirty minutes before the start of the experiment, 200–350 μL of a 1 g/mL barium sulfate ($BaSO_4$) aqueous suspension was diluted in 4 mL of DW and stirred vigorously (1500 rpm) in a glass vial for 2 min until a white cloudy suspension was obtained, resulting in concentrations of 50–87 mg/mL. Six hundred μL of the suspension was filled into the capsule, and the latter was fully locked. Then, 1 capsule at a time was administered to the dog orally without water, and X-ray images (CGO-2100 plus, Digital subtraction angiography, Wandong) were taken at the time of administration ($t = 0$ min), at 15 min, 30 min and then at 1, 1.5, 2, 2.5, 4, 6 and 8 h. Four hours after ingestion, the dog was given access to solid food and water. Feces, if excreted, were checked to detect intact or broken capsules. Three experiments per capsule group were performed. The dog was lightly anesthetized 10 min before every imaging time point with an intravenous injection of propofol (30–40 mg) to facilitate imaging. To remove the effect of circadian rhythm on transit, dosing was performed at the same time of the day. (all experiments were done with 1 dog). Opening time is described as the last time point where the capsule is seen on the X-rays.

### 2.12. Statistical analysis

Data analysis was carried out using Origin (Origin version 2021). Assuming a normal distribution of analyzed datasets, statistical tests included one-way analysis of variance (ANOVA) followed by Tukey's multiple comparisons test. The $p$ value threshold for statistical significance was set as 0.05.

## 3. Results and discussion

### 3.1. Screening, formulation selection and capsule characterization

In our work, commercially available hydroxypropyl methylcellulose (HPMC) capsules were used as molds to externally cast a thin hydrophobic coating (HC) of the EC layer followed by an enteric coating (EnC) of Eudragit S100 (Fig. 3).

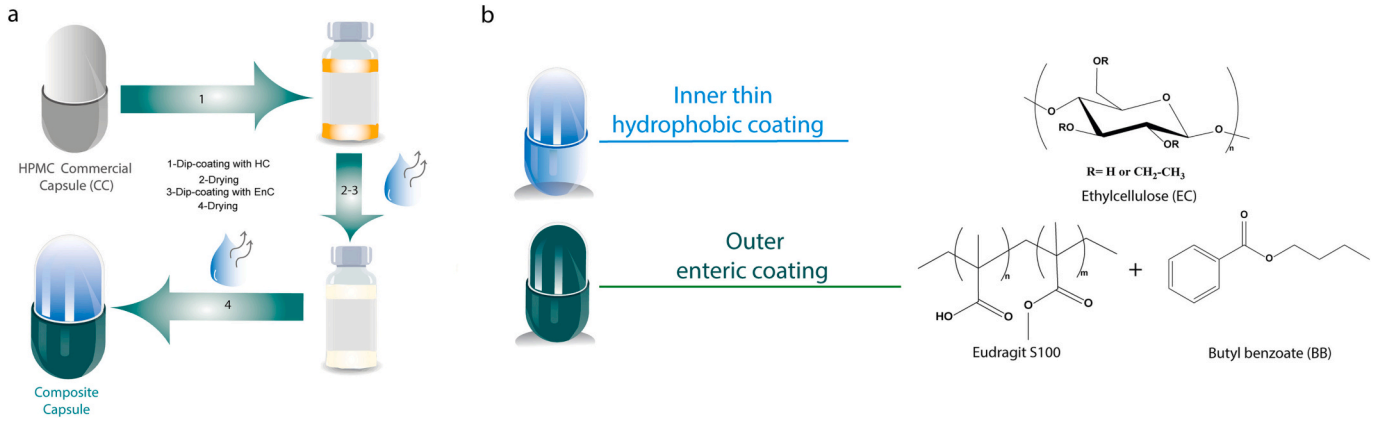


**Fig. 3.** Schematic illustration of the fabrication of the two optimized colonic capsules. A commercial capsule (CC) body and cap are dip-coated in HC solution and left to dry and the EnC is applied similarly on top of the HC, leading to the composite capsule (a). The composite capsule is made of an inner EC layer and an outer enteric coating, which is composed of Eudragit S100 and butyl benzoate (BB) (b).

The effects of different parameters, such as the dip-coating solvent, plasticizer type (hydrophobic or hydrophilic) and polymer concentration on various capsule properties were first assessed, and the data are reported and discussed in the Information section (Tables S1 and S2, and Figs. S1 and S2). Following this screening, two optimized capsule formulations, HC-1 EnC-1 and HC-2 EnC-2, whose compositions are provided in table S1, were fabricated. These 2 capsules differed in terms of their EC, Eudragit S100, and butyl benzoate (BB, plasticizer) concentrations. As displayed in Fig. 4a i and ii, the two optimized capsules were composed of a body and a cap with an embedded coni-snap shape, which when interlocked, allowed for the encapsulation of an Evans blue solution (Fig. 4a iii and iv). To confirm that the capsules coatings were hydrophobic enough to provide water resistance post filling, contact angle measurements were performed on each different layer (*i.e.*, HC and EnC) (Fig. 4b). Compared to the commercial HPMC capsule, which has a hydrophilic contact angle (CA) of 40.3°, HC-1 and HC-2 were more hydrophobic, with CAs of 96.7° and 101.3°, respectively. Regarding the external enteric coatings, EnC-1 and EnC-2 exhibited CAs of 87° and 95°, respectively. In addition, an initial screening was performed by filling capsules with an Evans blue solution and leaving them in contact with simulated gastric fluid (SGF) for 4 h. The capsules did not dissolve (Video S1), confirming the ability of the capsule layers to withstand internal and external water contact. This is essential for the encapsulation of aqueous bacterial suspensions, since compared to our system, hydrophilic capsules (such as HPMC and gelatin capsules) quickly dissolve (Video S2).

We next assessed the homogeneity as well as the thickness of the capsule coating layers by scanning electron microscopy (SEM) (Figs. 4c and d). The successful deposition of homogeneous hydrophobic layers (HC-1 and HC-2) by dip-coating was achieved, as depicted in Fig. 4c i and iii. By adding an external enteric coating (i.e EnC-1 or EnC-2), a second uniform film was created on the hydrophobic layer surface (Fig. 4c ii and iv). The HC-1 and HC-2 layers were *ca.* 15 μm thick, while the enteric coatings EnC-1 and EnC-2 had thicknesses of 15 and 7.5 μm, respectively. This difference in thickness might be related to the increase in BB concentration from 3 wt% in EnC-1 to 25 wt% in EnC-2 and could result in different mechanical support properties.

Next, the coated capsule shell (HC-1 EnC-1) was analyzed by 2D Raman mapping (Figs. 5a and b) to assess the film compositions and chemical homogeneity. The different polymer signals, corresponding to those of the individual layers of Eudragit S100, EC and HPMC, were identified by distinctive peaks at 1719, 244 and 289 $cm^{-1}$ (Fig. S5), respectively, which were tracked over a depth of 80 μm starting from the external capsule surface in steps of 10 μm. As shown in Fig. 5b, the Eudragit signal indicated that Eudragit represented the major component of the film over the first 30 μm, then the EC signal increased at over 20 μm and peaked at 30 μm. The overlap between the two composites corresponded to the region where both polymers (EC and S100) interpenetrated. Finally, at over 40 μm, HPMC represented the major shell component. These results agreed with the SEM thickness results as well as the results of the HPMC shell thickness (~120 μm). Then, the resistance of the coated capsules to proton diffusion was investigated in SGF (Fig. 5c). The pH of the encapsulated aqueous content of the capsules coated with only HC-1 and 2 decreased after 4 h by 0.84 and 0.67 units, respectively. This relatively low proton diffusion could be explained by the hydrophobicity of the EC layers, which restricts proton diffusion. [32]. With the addition of the enteric layers, the decrease in pH of the internal aqueous content was reduced to only 0.36 and 0.43 for HC-1 EnC-1 and HC-2 EnC-2, respectively, resulting in a final pH ~ 6.5 and increasing the shell resistance toward proton diffusion, which is important for ensuring maximal bacterial survival. Indeed, in gram-negative bacteria, the outer membrane does not act as a physical barrier to proton movement, as the porins are large enough to allow proton passage. In addition, under severe acid stress, the cytoplasmic pH drops to levels that cannot be corrected by buffering or ionic flux, resulting in low cell survival. [33]

Next, we assessed the diffusion of oxygen to determine whether the capsules would be suitable for the encapsulation of anaerobic bacteria. A colorimetric method was adapted for the quantification of aqueous dissolved oxygen from 0.05 to 0.297 ppm (Figs. 5d and S6 and Table S4). [34,35] When locked capsules containing an aqueous solution were left in contact with air, the dissolved oxygen levels increased from 0.15 to 0.23 ppm after 5 h for both capsules and reached equilibrium after *ca.* 24 h (0.30 ppm) (Fig. 5e). Next, we measured the dissolved oxygen content in the capsules after exposure to SGF for 2 h at 37 °C. As depicted in Fig. 5f, slightly lower dissolved oxygen concentrations were measured after contact with SGF at 37 °C compared to air (Fig. 5e). This could be explained by the solubility of $O_2$ in pure water and other fluids which decreases as the temperature increases [36]. Since many strict anaerobes that are present in the colon, such as *Bacteroides*, can tolerate these measured oxygen levels, [18,37] these results indicate that both capsules might be suitable for the encapsulation of some anaerobic bacterial strains provided that the capsules are administered a few hours after filling under $O_2$-free conditions.

Encouraged by these results, we proceeded with evaluating the capsules' stability under different GI conditions. First, we performed surface dissolution imaging (SDI) (Fig. 6a). The HC-1 EnC-1 or HC-2 EnC-2 capsules were fixed in a chamber in which SGF (pH 1.2) or simulated intestinal fluid (SIF) (pH 7.3) was circulated. The absorbance signal of BB (255 nm) in the buffer was quantified *via* video recording during exposure to the different GI tract fluids. The HC-1 EnC-1 capsules in SGF (Fig. 6b) showed no absorbance signal of BB in the dissolution

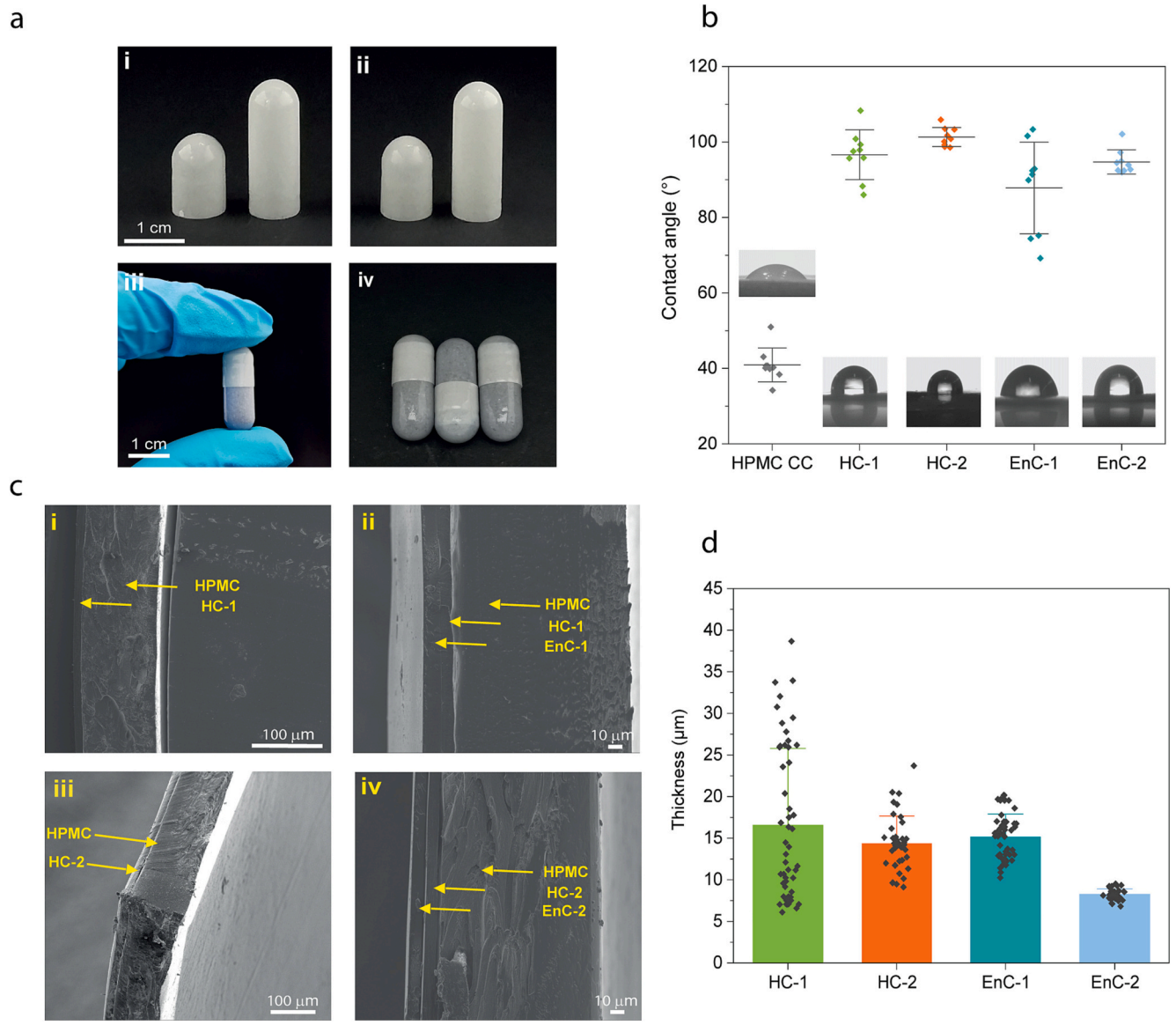


**Fig. 4.** Photographs (a) of HC-1 EnC-1 (i), HC-2 EnC-2 (ii) capsules, and HC-1 EnC-1 or HC-2 EnC-2 capsules filled with a solution of Evans blue (iii) (iv). Contact angles of the coating layers individually deposited on an HPMC commercial capsule (CC). Water droplet size: 7 µL (b). Means ± SDs ($n$ = 9). Cross-section SEM images (c) of HC-1 (i), EnC-1 deposited on HC-1 (ii), HC-2 (iii) and EnC-2 deposited on HC-2 (iv). The scales are 100, 10, 100 and 10 µm. Thicknesses of the HC-1, HC-2, EnC-1, and EnC-2 layers extracted from the SEM images (d). Means + SDs ($n$ = 34–51 measurements on 3 capsules per group). (For interpretation of the references to colour in this figure legend, the reader is referred to the web version of this article.)

solution when subjected to pH 1.2 over 2 h. However, when the HC-1 EnC-1 capsules were exposed to SIF (pH 7.3) simulating ileum conditions for 6 h, we observed a large increase in the absorbance of BB over the first hour, with an average maximum dissolution time of 0.38 h (Fig. 6c and Video S3). In addition, mechanical deformation of the capsules was observed (Fig. 6e i). This could be indicative of the rapid dissolution of the enteric coating at pH 7.3, causing the release of BB from the polymer matrix upon the deprotonation and dissolution of Eudragit S100. [38,39]

The same results were obtained for the HC-2 EnC-2 capsules in SGF (Fig. S7). However, once the capsules were subjected to SIF (pH 7.3), the signal of BB increased considerably with an average dissolution time of 0.60 h, which was 2 times longer than that of HC-1 EnC-1 (Fig. 6d). This 2-fold increase in the dissolution time of HC-2 EnC-2 could be explained by the higher hydrophobicity of the EnC-2 shell compared to that of the EnC-1 shell (Fig. 4b). The dissolution time of the enteric coatings in SIF (0.38 *vs.* 0.60 h for the HC-1 EnC1 and HC-2 EnC-2 capsules, respectively) suggested that the HC-1 EnC-1 capsule would lose its enteric coating more rapidly than the HC-2 EnC-2 capsule in the intestine, possibly leading to an earlier capsule opening.

### 3.2. *In vitro determination of the mechanical properties and opening of the capsules under different GI tract conditions*

Next, the pressure sensitivity of the capsules was characterized under simulated fasted-state GI conditions to evaluate their opening site. This pressure sensitivity was defined as the applied force necessary to cause the breakage or leakage of the capsule per area and calculated using eq. 1. Disintegration and mechanical compression tests were performed simultaneously to assess the effect of transit conditions on the capsule mechanical properties (Fig. 7a). Capsules containing an Evans blue solution were exposed to SGF at pH 1.2, followed by SIF at pH 6.8 or 7.3 for 3 and 6 h. These pH values and times were chosen since they are representative of the human small intestinal transit time and the pH of

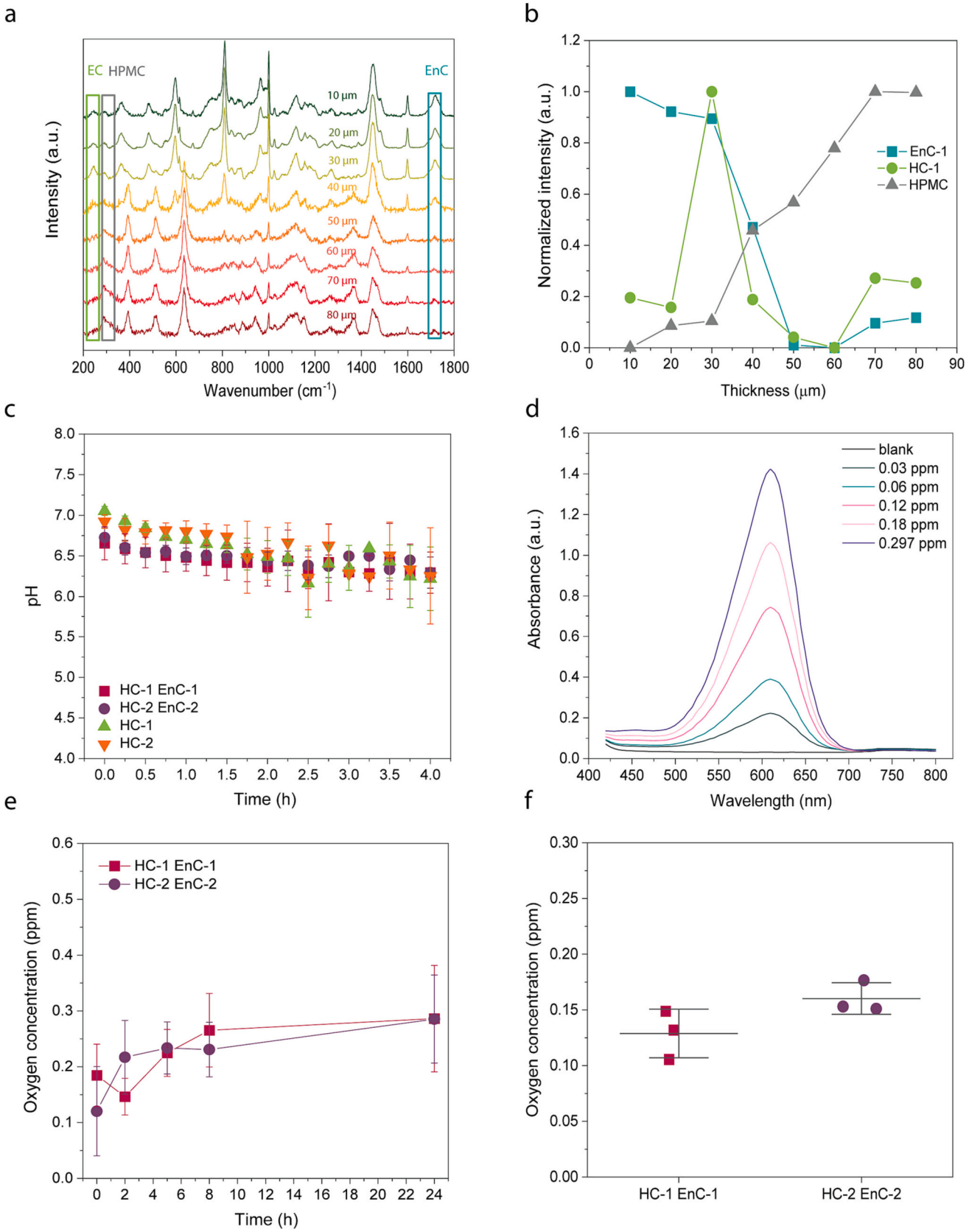


**Fig. 5.** Raman spectra of each mapping step (step size = 10 µm along the y direction) (a). Normalized Raman signal intensity *vs.* coating thickness. EnC-1, HC-1 and HPMC were quantified at 1719, 244 and 289 $cm^{-1}$, respectively (b). Change in pH values of the capsule contents during exposure to SGF (pH 1.2) over time (c). Means ± SDs ($n = 9$). Absorbance of indigo carmine between 420 and 800 nm as a function of aqueous dissolved oxygen content in ppm (d). Change in internal aqueous dissolved oxygen concentration in capsules HC-1 EnC-1 and HC-2 EnC-2 over time under atmospheric conditions (e) or after immersion in SGF for 2 h at 37 °C (f). Means ± SDs ($n = 3$). (For interpretation of the references to colour in this figure legend, the reader is referred to the web version of this article.)

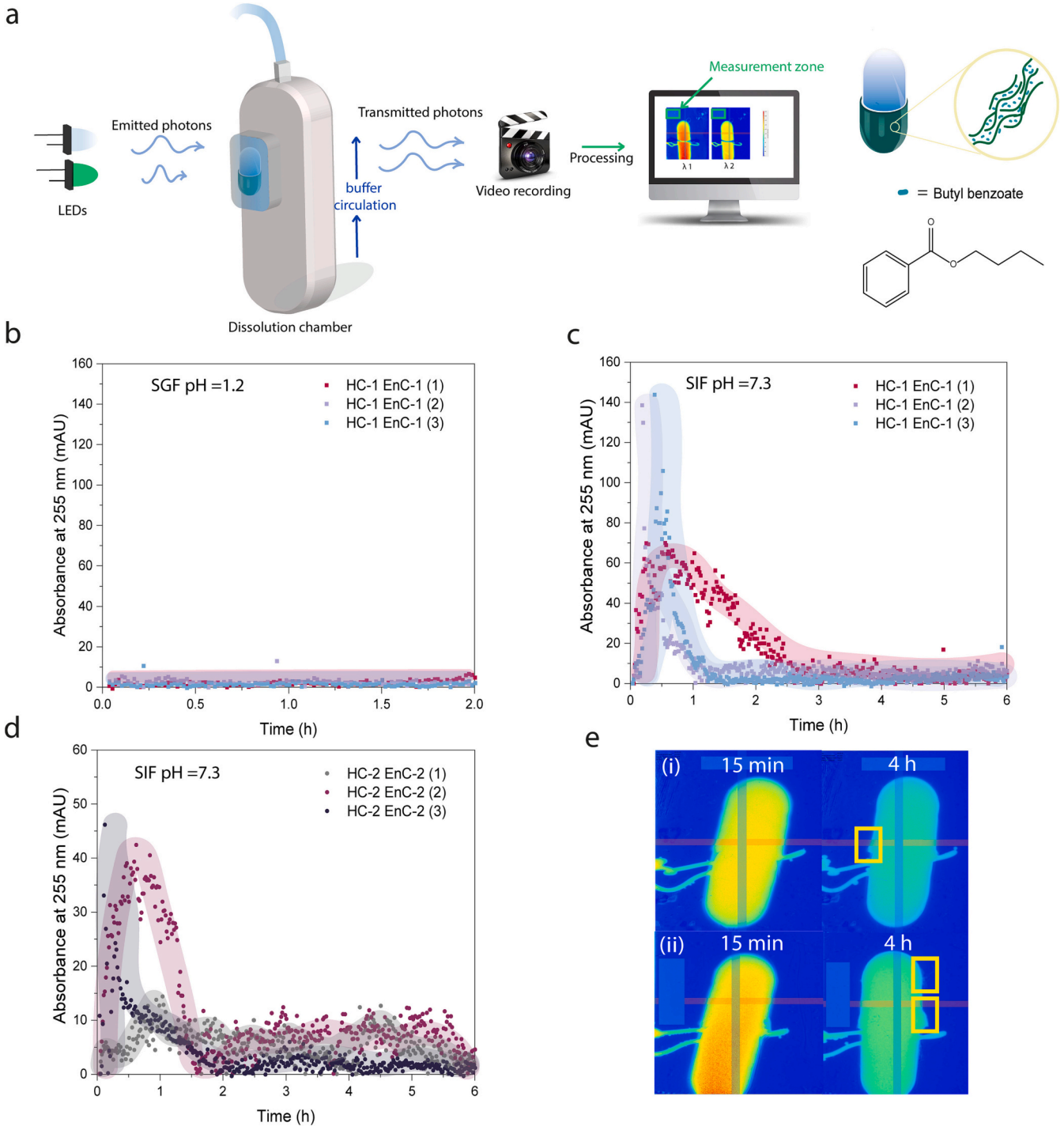


**Fig. 6.** Scheme describing the surface dissolution imaging system. Briefly, capsules are introduced in a dissolution chamber in which a fluid is run automatically in a closed loop. Light emitting diodes at 255 nm and 520 nm are used to image and video record the absorbance of BB as well as the visible object in real time. A processing step is used to convert the images to absorbance values (a). Absorbance levels of BB over time for the HC-1 EnC-1 capsules in SGF (b) and SIF 7.3 (c) ($n$ = 3). Absorbance values of BB over time for the HC-2 EnC-2 capsules in SIF 7.3 (d). UV-Images of the capsules after 15 min and 4 h (e) for the HC-1 EnC-1 (i) and HC-2 EnC-2 (ii) capsules in SIF 7.3. Yellow squares indicate mechanical deformation of the capsules. (For interpretation of the references to colour in this figure legend, the reader is referred to the web version of this article.)

the proximal and distal intestinal segments. [40] In a follow-up experiment, the same transit steps were used, but bile acids and lecithin were introduced in the first 3 h of SIF exposure to better simulate the duodenum and jejunum environment in terms of dissolution properties. [41] However, these additives were later removed in the second step (exposure between 3 and 6 h) as they are primarily hydrolyzed and reabsorbed in the distal portion of the small intestine. The initial pressure-at-break ($P_b$) of the HC-1 EnC-1 and HC-2 EnC-2 capsules were 1200 and 710 mbar, respectively (Figs. 7b and c). The initial difference in mechanical strength between the two capsules could be explained by the difference in the composition of the layers, including a lower EC concentration (6.6 *vs.* 4.5 wt%, respectively) and a higher plasticizer concentration (3 *vs.* 25 wt%, respectively) for HC-2 EnC-2 capsules. After 2 h in SGF (pH 1.2), the $P_b$ dropped to 810 and 380 mbar for the

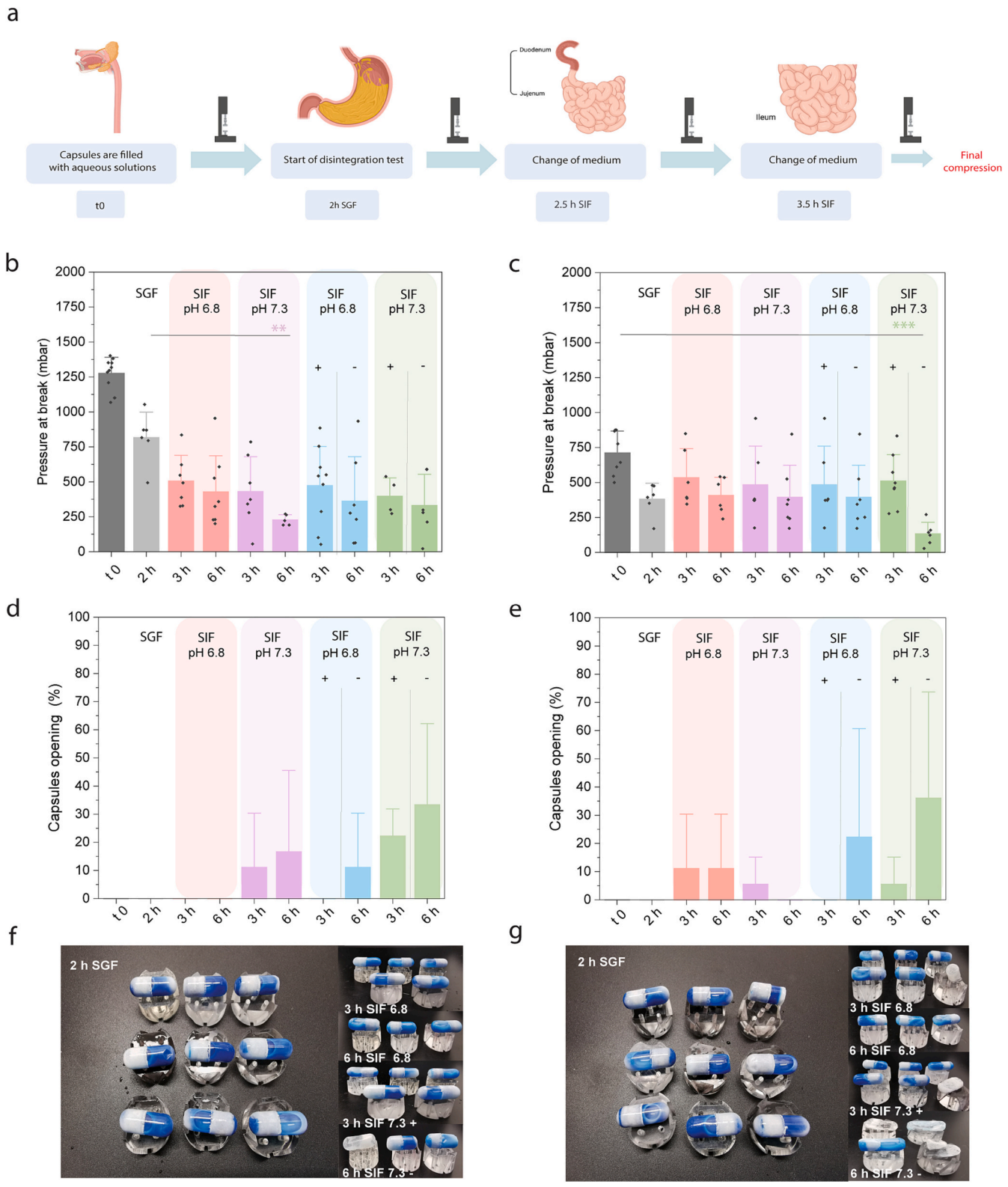


**Fig. 7.** Schematic illustration representing disintegration tests coupled with mechanical compression. The capsules filled with an aqueous solution of Evans blue and subsequently tested for their pressure-at-break post filling ($t_0$), in SGF for 2 h and then in SIF at pH = 6.8 or 7.3 for 2.5 h with or without bile acids and lecithin. Finally, bile and lecithin are removed, and the capsules are immersed in SIF at pH 6.8 or 7.3 for 3.5 h. After each GI test condition, the pressure-at-break of the capsules is tested with a compression test (a). Pressure-at-break of the HC-1 EnC-1 capsule (b) and the HC-2 EnC-2 capsule (c). Means + SDs ($n = 3$). Capsule opening per step in % of the HC-1 EnC-1 (d) and HC-2 EnC-2 (e) capsules ($n = 8$–18 capsules). The sign (+) designates the presence of bile acids and lecithin. The sign (−) designates the removal of bile acids and lecithin. Photographs of the HC-1 EnC-1 (f) and HC-2 EnC-2 (g) capsules containing an Evans blue solution after different steps. (n = 3). n indicates the number of independent experiments. Statistical significance was calculated using ordinary one-way ANOVA followed by Tukey's multiple comparisons test and is depicted as ** $p < 0.01$ and *** $p < 0.001$. Fig. 7a was created with BioRender. (For interpretation of the references to colour in this figure legend, the reader is referred to the web version of this article.)

HC-1 EnC-1 and HC-2 EnC-2 capsules, respectively (Figs. 7b and c), which can be explained by the dissolution of the HPMC inner shell upon the encapsulation of the aqueous solution. The higher $P_b$ of the HC-1 EnC-1 capsule was found to be more promising since this mechanical strength could allow the capsules to withstand high pressure spikes that might occur in some occasions in the stomach (*i.e.*, 200–400 mbar), thus preventing their early opening. However, it is worth mentioning, that in fasted human volunteers, these spikes were absent in 45% of the volunteers and that pressures below 100 mbar were observed accompanied by a rapid gastric transit [42]. As reported by Koziolek et al., capsules might face minimal resistance during fasting since the pylorus is open, and those high-pressure spikes might be experienced when the dosage form is pushed against a closed pylorus by peristaltic waves [43] . We also observed that, post disintegration in SGF, all capsule types remained intact, and no opening (Figs. 7d and e), leakage or deformation was observed (Figs. 7f and g). These results suggest that all capsule types could resist disintegration in the gastric environment and retain their encapsulated aqueous content.

After exposure to SIF (pH 6.8, without bile acids and lecithin), a further decrease in $P_b$ was observed for the HC-1 EnC-1 capsules over time ($P_b = 500$ and 400 mbar for 3 and 6 h, respectively). This could be due to the swelling of Eudragit S100 caused by the partial deprotonation of carboxylic groups at higher pH. Moreover, no capsules opened under these conditions (Figs. 7d and f and Table S5). In contrast, almost no change in the mechanical properties of the HC-2 EnC-2 capsules was noted under these conditions, and similar $P_b$ values were recorded after 3 and 6 h (Fig. 7c). Nevertheless, ~13% of the capsules opened after 3 and 6 h (Figs. 7e, g and Table S6).

After exposure to neutral intestinal fluid (pH 7.3), a significant decrease in $P_b$ was observed for the HC-1 EnC-1 capsules after 6 h (230 mbar). Moreover, capsule opening increased to ~14%. This could be explained by the entire dissolution of the EnC-1 layer, which decreased the mechanical strength of the capsules. On the other hand, increasing the pH did not affect the mechanical properties or opening of the HC-2 EnC-2 capsules. Indeed, the capsules maintained the same $P_b$ as that of the same type of capsule that had been exposed to a lower pH (6.8).

Exposure to the SIF pH 6.8 (+) (with the addition of bile acids and lecithin) to mimic intestinal fluids under fasted state did not change the mechanical strength of both capsule types over 6 h compared to exposure to the SIF pH 6.8 without bile acids and lecithin. However, we noticed an increase in capsule opening of ~12% and 22% for the HC-1 EnC-1 and HC-2 EnC-2 capsules, respectively. In contrast, increasing the pH to 7.3 (+) in the presence of bile acids and lecithin had a significant effect only on HC-2 EnC-2 capsules, decreasing its mechanical properties after 6 h, to reach a $P_b$ of 130 mbar. This decrease correlates to the observed increase in capsule opening (~40%). This could have resulted from the high butyl benzoate content in the EnC-2 layer, which could increase the dissolution of EnC-2 in the presence of bile and lecithin at a pH >7. [44] Despite the lack of change in the mechanical properties of the HC-1 EnC-1 capsules under these conditions, a higher capsule opening was also recorded (~33%).

Based on these results, we found that the pressure sensitivity of the capsules was dependent on different GI test conditions. The HC-1 EnC-1 capsules were more sensitive to pH increase, while the HC-2 EnC-2 capsules were affected by the presence of bile acids and lecithin during transit. All capsules were found to be likely to survive transit in the small intestine, in which the pressure can reach a maximum of 100 mbar (±65 mbar) in humans. However, the HC-2 EnC-2 capsules have a higher chance of opening in the colon, in which the pressure can reach 140 mbar (±75 mbar).

Next, we encapsulated live aqueous bacterial suspensions and assessed the efficacy of the capsules to protect the bacteria from simulated GI fluids.

### 3.3. Encapsulation of live aqueous bacterial suspension and viability assessment

First, we cultured a mixture of aerobic bacterial strains that have been reported to potentially confer health benefits [45–47] (*E. faecium*, *L. plantarum*, *L. rhamnosus* and *L. acidophilus*) and subjected this saturated bacterial suspension to saline (0.85%) and 70% IPA to produce 2 populations of live and dead bacterial cells distinguishable by flow cytometry (Fig. S8). Next, the aqueous suspension of this saturated live bacterial mixture was subjected to SGF at a pH 1.2, 3 and 5 for 2 h, SIF pH 6.8 (+) (with bile acids and lecithin) for 2.5 h or saline and 70% IPA for 1 h at 37 °C (live and dead control). From Fig. 8a, it can be seen that the bacterial mixture remained viable in saline and in SGF with pH of 3 and 5. However, the viability decreased drastically at pH 1.2, in SIF 6.8 (+) and after exposure to 70% IPA. This could indicate that low gastric pH as well as the presence of intestinal bile could be detrimental to bacterial survival. We then tested the ability of the capsules to protect live bacteria by exposing them to SGF 1.2 for 2 h and SIF 6.8 (+) for 2.5 h and finally assessing bacterial viability after each step. The bacterial viability remained very high in both HC-1 EnC-1 and HC-2 EnC-2 capsules (94 and 95%, respectively) post SGF 1.2 exposure (Fig. 8b). The same high viability (~98%) was also observed after exposure to SIF 6.8 (+). This confirmed the ability of our capsules to equally protect live bacteria in aqueous suspensions from the low gastric pH as well as intestinal bile acids.

Next, we assessed the ability of the capsules to protect live symbiont obligate anaerobes, namely *B. thetaiotaomicron,* a major commensal of the human microbiota belonging to the Bacteroides phylum, beneficial for host physiology and immunity [48]. As observed in Figs. 8c and d as well as Fig. S9, *B. thetaiotaomicron* cells remained highly viable when encapsulated in HC-1 EnC-1 and HC-2 EnC-2 capsules with 94 and 74% viability, respectively, after subsequent exposure to SGF 1.2 for 2 h and SIF 6.8 (+) for 2.5 h. It was also observed that 20% of live bacteria encapsulated in HC-2 EnC-2 were dying after 4.5 h exposure to the simulated GI fluids. This difference in viability between the two capsule types might be due to the faster $O_2$ diffusion in HC-2 EnC-2 capsules leading to a higher dissolved molecular oxygen $O_2$ concentration (Figs. 5e and f).

Nonetheless, this demonstrates the ability of the capsules to encapsulate potential obligate anaerobes and keeping cells highly viable for up to 4.5 h, which is enough time to reach the ileum where the oxygen partial pressure in the lumen would decrease sharply. [49].

Next, we moved on to test the opening of our capsules *in vivo* in the canine model. Despite higher pressure events during canine gastric transit (800 mbar) compared to those during human gastric transit, the similar average intestinal pressures imply that this model is suitable for evaluating the mechanical resilience of oral solid dosage forms and was therefore used in the subsequent experiments. [50]

### 3.4. In vivo imaging study

To determine the opening time of the capsules and their ability to deliver aqueous content to the colon *in vivo*, aqueous suspensions of $BaSO_4$ of varying concentrations were encapsulated in the HC-1 EnC-1 and HC-2 EnC-2 capsules, and their disintegration patterns were studied. This study was optimized to ensure that $BaSO_4$ did not affect capsule disintegration and opening. As shown in Fig. S10 and Video S4, the capsules with 8.75 wt% $BaSO_4$ aqueous suspensions behaved like control capsules containing a solution of Evans blue. Thus, these capsules were administered orally in a beagle dog model.

The dogs were fasted for 12 h with unrestricted access to water since it slightly promotes gastric juice secretion. [50,51] After administration of the capsule, water and food were restricted and X-ray images of the capsules transit were taken at different time intervals. A solid meal was provided after 4 h to activate the ileocecal reflex, which promotes the movement of undigested intestinal contents through the ileocolic orifice

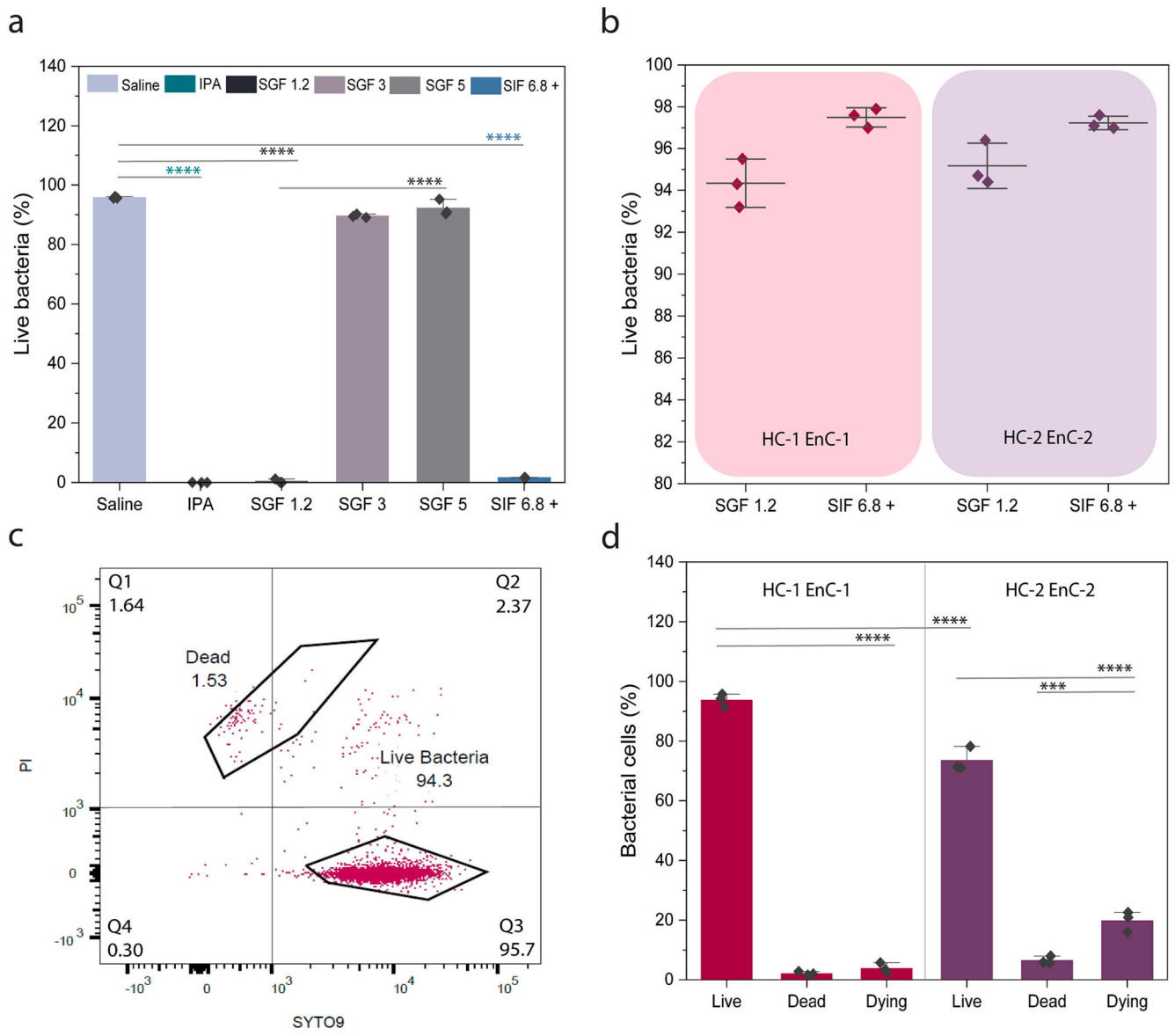


**Fig. 8.** Viability of mixture of bacterial cells (%) post exposure to saline, IPA, SGF at a pH 1.2, 3 and 5, SIF pH 6.8 (+) assessed by flow cytometry (a). Viability of mixture of bacterial cells (%) encapsulated in HC-1 EnC-1 and HC-2 EnC-2 post subsequent exposure to SGF 1.2 for 2 h and SIF 6.8 (+) for 2.5 h using flow cytometry (b). Means ± SDs ($n = 3$). Example of density plot of *B. thetaiotaomicron* cells where Q1 designates the dead population, Q2 the dying population, Q3 the live population and Q4 the unstained population by flow cytometry (c). Other replicates are provided in fig. S9. Percentage of live, dead, and dying *B. thetaiotaomicron* cells post encapsulation and subsequent exposure to SGF 1.2 for 2 h and SIF 6.8 (+) at 37 °C (d). Means ± SDs (n = 3). Statistical significance was calculated using ordinary one-way ANOVA followed by Tukey's multiple comparisons test and is depicted as *** $p < 0.001$ and **** $p < 0.0001$.

and into the colon. [42,52] As shown in Figs. 9b, c and S11, the HC-1 EnC-1 and HC-2 EnC-2 capsules appeared to open *ca.* 3.3 and 4.3 h post administration, respectively. However, the opening time was variable, as indicated by the individual values shown in fig. S11. No intact capsules were recovered in the feces, confirming their opening in the GI tract, likely in the distal segment. Indeed, beagle dogs in a fasted state have a short gastric emptying time of 0.57 h (±0.37 h) and a consistent small intestinal transit time of 1–2 h. [50] Previous studies have suggested that pressure-sensitive capsules that open approximately 3.5 h after ingestion by beagle dogs in the fasted state are likely to be in the colon. [30] Considering this, the HC-2 EnC-2 capsules were assumed to probably be more suitable than the HC-1 EnC-1 capsules for delivering bacteria as they approach the colon, since 2/3 of the former and only 1/3 of the latter opened after 3.5 h. *In vitro*, we demonstrated that the capsules opened at colonic arrival times (6–8 h). To ensure the relevance of our findings to humans, the fasted beagle dog model was chosen due to its similarity in gastric emptying time and constant intestinal transit time when compared to fasted humans. However, the difference in capsule time opening observed *in vivo* might be attributed to several factors specific to the canine GI tract, which include a higher rate of bile secretion, elevated gastric and intestinal mechanical pressure spikes (reaching up to 800 and 200 mbar in the stomach and intestine, respectively), and higher gastric and intestinal pH levels compared to fasted humans. These unique physiological conditions in the canine GI tract likely contributed to the faster disintegration of the capsules in the *in-vivo* setting. [50,53]

## 4. Conclusion

In this study, we developed two colonic capsules (HC-1 EnC-1 and HC-2 EnC-2) that could encapsulate aqueous media and provide protection against gastric acidity and, to some extent, oxygen. Relatively

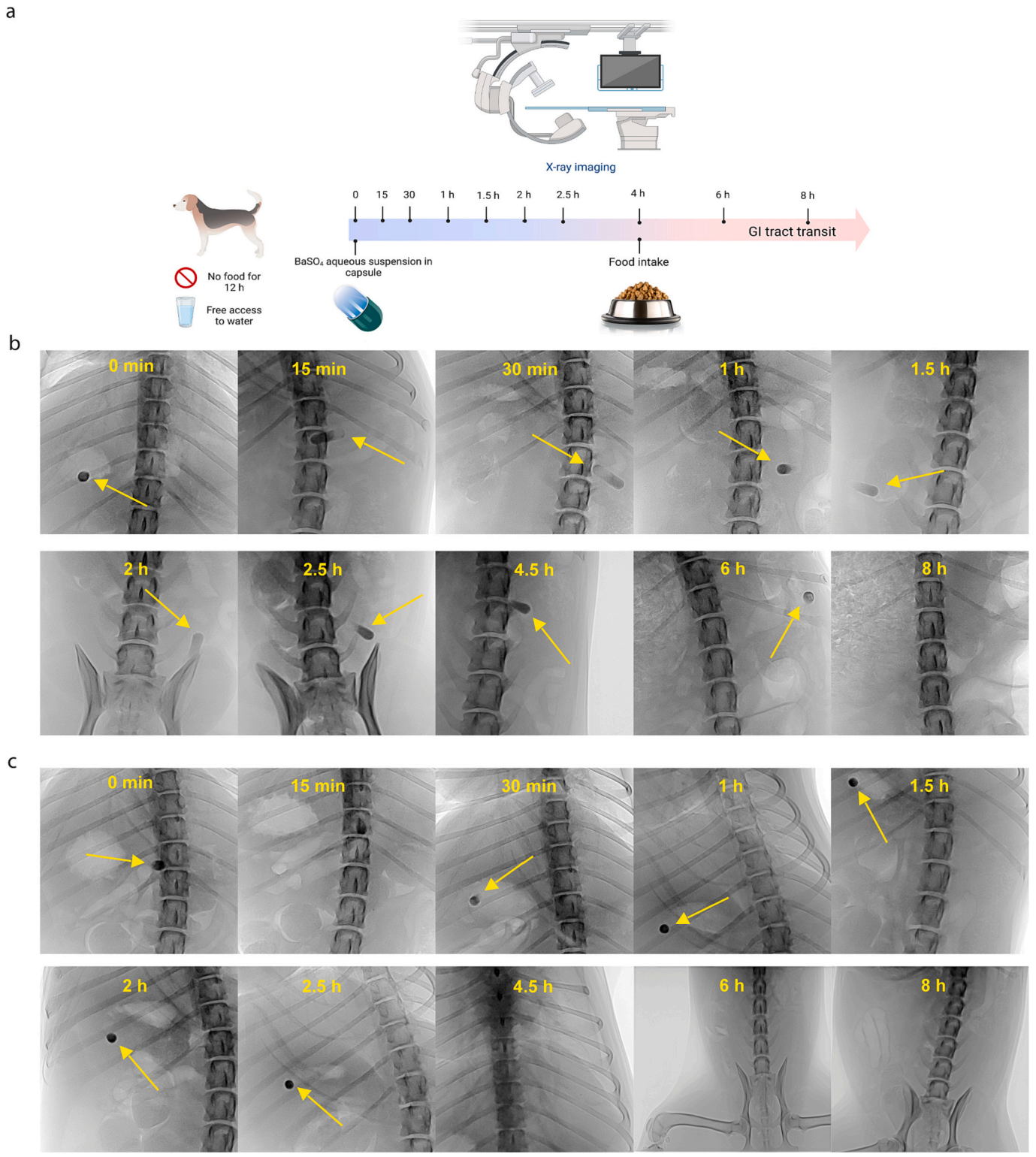


**Fig. 9.** Schematic illustration of the *in vivo* protocol: briefly, beagle dogs are fasted for 12 h with free access to water. HC-1 EnC-1 or HC-2 EnC-2 capsules were then filled with $BaSO_4$ aqueous suspension, and a meal was provided 4 h after capsule administration. X-ray images from ventral, dorsal and side views were taken at 0 min, 15 min, 30 min, 1, 1.5, 2, 2.5, 4, 6 and 8 h after capsule administration (a) to track the transit of the HC-1 EnC-1 (b) and HC-2 EnC-2 (c) capsules in the GI tract. The capsule position is indicated with a yellow arrow. A representative capsule of each group is shown here, and other replicates are provided in fig. S11. Part a of Fig. 9 was created with BioRender. (For interpretation of the references to colour in this figure legend, the reader is referred to the web version of this article.)

low oxygen diffusion rates could allow the extemporaneous preparation and administration of anaerobic bacterial strains, at least under research conditions. *In vitro* testing confirmed that the capsules were mechanically strong enough to survive transit through the stomach as well as the upper and proximal small intestinal segments. The encapsulation of a mixture of aerobic strains as well as anaerobic commensals in our capsules and its exposure to simulated harsh GI conditions showcased the ability of the capsules to protect the bacteria (viability 74–98%). *In vivo*

studies with a beagle dog model suggested that 67% of the HC-2 EnC-2 capsules likely opened in the ileum/colon. The HC-1 EnC-1 capsules, on the other hand, opened sooner. The development of colonic capsules encapsulating suspended live microorganisms could prove useful for rapidly screening microbial therapeutics and eventually simplifying their dosing regimen by delivering a greater fraction of viable bacteria to the colon compared to dry formulations. In this respect, further studies should aim to evaluate the efficacy of these capsules for protecting and delivering live bacteria *in vivo*. In addition, releasing an aqueous medium in the distal GI tract could also be exploited for the administration of biologics that are sensitive to lyophilization or spray-drying.

Supplementary data to this article can be found online at https://doi.org/10.1016/j.jconrel.2023.11.048.

## Author contributions

A.F. engineered and conducted the experiments, analyzed, interpreted the data and co-wrote the manuscript. M.G.B developed the oxygen quantification method and reviewed the data and the manuscript. N.Z developed aerobic bacterial culture protocols. Z.L monitored the *in-vivo* experiments. J.C.L. supervised the project, interpreted the data, and co-wrote the manuscript.

## Funding

This work was financially supported by a grant from the Swiss National Science Foundation (grant 315230_197644/1).

## Declaration of generative AI and AI-assisted technologies in the writing process

During the preparation of this work the author(s) used ChatGPT in order to rephrase certain sentences. After using this tool, the author(s) reviewed and edited the content as needed and take full responsibility for the content of the publication.

## CRediT authorship contribution statement

**Fatma Abdi:** Writing – review & editing, Writing – original draft, Visualization, Validation, Methodology, Investigation, Formal analysis, Data curation, Conceptualization. **Marina Green Buzhor:** Writing – review & editing, Validation, Supervision, Methodology, Formal analysis. **Nadia Zellweger:** Methodology. **Zhi-Luo:** Funding acquisition, Conceptualization. **Jean-Christophe Leroux:** Writing – review & editing, Validation, Supervision, Resources, Project administration, Funding acquisition, Conceptualization.

## Declaration of Competing Interest

The authors declare that they have no competing interests.

## Data availability

The data that support the findings of this study are available in the supplementary material of this article.

## Acknowledgements

We would like to thank the Scientific Center for Optical and Electron Microscopy (ScopeM) of ETH Zurich for providing helpful technical advice. The authors thank Dr. Sung Sik Lee (ScopeM, Department of Health Sciences and Technology, ETH Zurich, Switzerland) for his support and assistance in Raman mapping. The authors thank Dr. Malgorzata Kisielow for her assistance in flow cytometry. The authors thank Prof. Emma Slack as well as Giorgia Greter for providing and assisting with culturing the *B. thetaomicron* strain.

## References

[1] P.D. Cani, Gut microbiota — at the intersection of everything? Nat. Rev. Gastroenterol. Hepatol. 14 (6) (2017) 321–322.
[2] C.B. Lambring, et al., Impact of the microbiome on the immune system 39 (5) (2019) 313–328.
[3] Y. Fan, O. Pedersen, Gut microbiota in human metabolic health and disease, Nat. Rev. Microbiol. 19 (1) (2021) 55–71.
[4] E.N. Baruch, et al., Fecal microbiota transplant promotes response in immunotherapy-refractory melanoma patients, Science 371 (6529) (2021) 602–609.
[5] S. Khanna, et al., Efficacy and safety of RBX2660 in PUNCH CD3, a phase III, randomized, double-blind, placebo-controlled trial with a Bayesian primary analysis for the prevention of recurrent Clostridioides difficile infection, Drugs 82 (15) (2022) 1527–1538.
[6] N.M.J. Hanssen, W.M. de Vos, M. Nieuwdorp, Fecal microbiota transplantation in human metabolic diseases: from a murky past to a bright future? Cell Metab. 33 (6) (2021) 1098–1110.
[7] M. Gulati, et al., Delivery routes for faecal microbiota transplants: available, anticipated and aspired, Pharmacol. Res. 159 (2020), 104954.
[8] S. Bellali, et al., A new protectant medium preserving bacterial viability after freeze drying, Microbiol. Res. 236 (2020), 126454.
[9] L.E. Papanicolas, et al., Bacterial viability in faecal transplants: which bacteria survive? EBioMedicine 41 (2019) 509–516.
[10] J. Wolfe, G. Bryant, Freezing, drying, and/or Vitrification of Membrane–Solute–Water Systems, Cryobiology 39 (2) (1999) 103–129.
[11] K. Vorländer, et al., Along the process chain to probiotic tablets: evaluation of mechanical impacts on microbial viability, Pharmaceutics 12 (1) (2020) 66.
[12] E. Byl, et al., Importance of pressure plasticity during compression of probiotic tablet formulations, Eur. J. Pharm. Biopharm. 145 (2019) 7–11.
[13] A.R. Fassihi, M.S. Parker, Inimical effects of compaction speed on microorganisms in powder systems with dissimilar compaction mechanisms, J. Pharm. Sci. 76 (6) (1987) 466–470.
[14] S. Li, et al., Oral delivery of bacteria: basic principles and biomedical applications, J. Control. Release 327 (2020) 801–833.
[15] J.-C. Rambaud, et al., Manipulation of the human gut microflora, Proc. Nutr. Soc. 52 (2) (1993) 357–366.
[16] P. Raibaud, R. Ducluzeau, Etude de la colonisation bactérienne du tractus gastro-intestinal à l'aide de modèles expérimentaux, Rev. Scient. Tech. (Intern. Off. Epizoot.) 8 (2) (1989) 361–373.
[17] M.T. Cook, et al., Microencapsulation of probiotics for gastrointestinal delivery, J. Control. Release 162 (1) (2012) 56–67.
[18] W.J. Loesche, Oxygen sensitivity of various anaerobic Bacteria, Appl. Microbiol. 18 (5) (1969) 723–727.
[19] P. Feuerstadt, et al., SER-109, an oral microbiome therapy for recurrent clostridioides difficile, Infection. 386 (3) (2022) 220–229.
[20] H.A. Hong, L.H. Duc, S.M. Cutting, The use of bacterial spore formers as probiotics, FEMS Microbiol. Rev. 29 (4) (2005) 813–835.
[21] M.T. Cook, et al., Production and evaluation of dry alginate-chitosan microcapsules as an enteric delivery vehicle for probiotic bacteria, Biomacromolecules 12 (7) (2011) 2834–2840.
[22] N. Huyghebaert, et al., Development of an enteric-coated formulation containing freeze-dried, viable recombinant Lactococcus lactis for the ileal mucosal delivery of human interleukin-10, Eur. J. Pharm. Biopharm. 60 (3) (2005) 349–359.
[23] H.P. Browne, et al., Culturing of 'unculturable' human microbiota reveals novel taxa and extensive sporulation, Nature 533 (7604) (2016) 543–546.
[24] A. Rakotonirina, T. Galperine, E. Allémann, Fecal microbiota transplantation: a review on current formulations in Clostridioides difficile infection and future outlooks, Expert. Opin. Biol. Ther. 22 (7) (2022) 929–944.
[25] Z. Hu, et al., New preparation method of intestinal pressure-controlled colon delivery capsules by coating machine and evaluation in beagle dogs, J. Control. Release 56 (1) (1998) 293–302.
[26] T. Takaya, et al., Importance of dissolution process on systemic availability of drugs delivered by colon delivery system, J. Control. Release 50 (1) (1998) 111–122.
[27] T. Takaya, et al., Development of a colon delivery capsule and the pharmacological activity of recombinant human granulocyte colony-stimulating factor (rhG-CSF) in beagle dogs, J. Pharm. Pharmacol. 47 (6) (1995) 474–478.
[28] K. Matsuda, et al., Effect of food intake on the delivery of fluorescein as a model drug in colon delivery capsule after oral administration to beagle dogs, J. Drug Target. 4 (2) (1996) 59–67.
[29] N. Shibata, et al., Application of pressure-controlled colon delivery capsule to oral administration of glycyrrhizin in dogs, J. Pharm. Pharmacol. 53 (4) (2001) 441–447.
[30] Y.-I. Jeong, et al., Evaluation of an intestinal pressure-controlled colon delivery capsules prepared by a dipping method, J. Control. Release 71 (2) (2001) 175–182.
[31] J.T. Collins, A. Nguyen, M. Badireddy, Anatomy, abdomen and pelvis, small intestine, in: StatPearls, StatPearls Publishing, Treasure Island (FL), 2017.
[32] S.A. Fischer, B.I. Dunlap, D. Gunlycke, Correlated dynamics in aqueous proton diffusion, Chem. Sci. 9 (35) (2018) 7126–7132.
[33] P. Lund, A. Tramonti, D. De Biase, Coping with low pH: molecular strategies in neutralophilic bacteria, FEMS Microbiol. Rev. 38 (6) (2014) 1091–1125.
[34] W.J.A.C. Loomis, Rapid microcolorimetric determination of dissolved oxygen 26 (2) (1954) 402–404.
[35] E. Narita, F. Lawson, K.J.H. Han, Solubility of oxygen in aqueous electrolyte solutions 10 (1) (1983) 21–37.

[36] W. Xing, et al., 1 - oxygen solubility, diffusion coefficient, and solution viscosity, in: W. Xing, G. Yin, J. Zhang (Eds.), Rotating Electrode Methods and Oxygen Reduction Electrocatalysts, Elsevier, Amsterdam, 2014, pp. 1–31.
[37] M.K. Bacic, C.J. Smith, Laboratory maintenance and cultivation of bacteroides species, Curr. Protoc. Microbiol. 9 (1) (2008), p. 13C. 1.1-13C. 1.21.
[38] S. Rehman, et al., Fabrication, evaluation, in vivo pharmacokinetic and toxicological analysis of pH-sensitive eudragit S-100-coated hydrogel beads: a promising strategy for colon targeting, AAPS PharmSciTech 22 (2021) 1–17.
[39] E.L. McConnell, M.D. Short, A.W. Basit, An in vivo comparison of intestinal pH and bacteria as physiological trigger mechanisms for colonic targeting in man, J. Control. Release 130 (2) (2008) 154–160.
[40] M. Koziolek, et al., Investigation of pH and temperature profiles in the GI tract of fasted human subjects using the Intellicap® system 104 (9) (2015) 2855–2863.
[41] E. Söderlind, et al., Simulating fasted human intestinal fluids: understanding the roles of lecithin and bile acids, Mol. Pharm. 7 (5) (2010) 1498–1507.
[42] F. Schneider, et al., Resolving the physiological conditions in bioavailability and bioequivalence studies: comparison of fasted and fed state, Eur. J. Pharm. Biopharm. 108 (2016) 214–219.
[43] M. Koziolek, et al., Navigating the human gastrointestinal tract for oral drug delivery: uncharted waters and new frontiers, Adv. Drug Deliv. Rev. 101 (2016) 75–88.
[44] V.I. Reshetnyak, Physiological and molecular biochemical mechanisms of bile formation, World J Gastroenterol: WJG 19 (42) (2013) 7341.
[45] J. Ghyselinck, et al., A 4-strain probiotic supplement influences gut microbiota composition and gut wall function in patients with ulcerative colitis, Int. J. Pharm. 587 (2020), 119648.
[46] M.E. Segers, S. Lebeer, Towards a better understanding of lactobacillus rhamnosus GG - host interactions, Microb. Cell Factories 13 (1) (2014) S7.
[47] M.J. Foysal, et al., Lactobacillus acidophilus and L. plantarum improve health status, modulate gut microbiota and innate immune response of marron (Cherax cainii), Sci. Rep. 10 (1) (2020) 5916.
[48] J.L. Sonnenburg, et al., Glycan foraging in vivo by an intestine-adapted bacterial symbiont 307 (5717) (2005) 1955–1959.
[49] J.-Y. Lee, R.M. Tsolis, A.J. Bäumler, The microbiome and gut homeostasis 377 (6601) (2022) p. eabp9960.
[50] M. Koziolek, et al., Characterization of the GI transit conditions in beagle dogs with a telemetric motility capsule, Eur. J. Pharm. Biopharm. 136 (2019) 221–230.
[51] K. McArthur, D. Hogan, J.I. Isenberg, Relative stimulatory effects of commonly ingested beverages on gastric acid secretion in humans, Gastroenterology 83 (1, Part 2) (1982) 199–203.
[52] J, I.A, Seventh annual graduate fortnight:“diseases of the gastrointestinal tract,” October 22 to November 2, 1934: The Wesley M. carpenter lecture, Appl. Physiol. Gastro-Intest. Innerv. 10 (11) (1934) 643.
[53] P.L. Walsh, et al., Comparing dog and human intestinal fluids: implications on solubility and biopharmaceutical risk assessment, AAPS PharmSciTech 18 (2017) 1408–1416.